ESC European Society of Cardiology

European Heart Journal - Imaging Methods and Practice (2024) **2**, qyae085
https://doi.org/10.1093/ehjimp/qyae085

REVIEW

Role of 3D transoesophageal echocardiography in the study of infective endocarditis. Demonstration in a case collection

Roberto Baltodano-Arellano [1,2], Daniel Huaman-Carrasco [3], Kelly Cupe-Chacalcaje [2], Angela Cachicatari-Beltran [2], Lindsay Benites-Yshpilco [4], Dante Urdanivia-Ruiz [2], Eliana Rafael-Horna [2,*], Luis Falcón-Quispe [2], Alessio Demarini-Orellana [5], Kevin Velarde-Acosta [4], Xochitl Ortiz-Leon [6], and Gerald Levano-Pachas [3]

[1]School of Medicine, Universidad Nacional Mayor de San Marcos, Lima, Peru
[2]Cardiac Imaging Area of Cardiology Service, Hospital Guillermo Almenara Irigoyen—EsSalud, Lima, Peru
[3]Cardiology Service, Hospital Guillermo Almenara Irigoyen—EsSalud, Lima, Peru
[4]Resident of Cardiology Service, Hospital Guillermo Almenara Irigoyen—EsSalud, Lima, Peru
[5]School of Medicine, Universidad San Martin de Porres, Lima, Peru
[6]Echocardiography Department, Instituto Nacional de Cardiología Ignacio Chavez, Ciudad de México, Mexico

Received 9 May 2024; accepted after revision 10 August 2024; online publish-ahead-of-print 20 August 2024

Infective endocarditis (IE) is a condition that predominantly affects native or prosthetic heart valves, which is currently on the rise due to the increase in invasive cardiology procedures, such as the utilization of cardiac implantable electronic devices and transcatheter interventions. The recommended imaging tests for diagnosis are 2D transthoracic echocardiography (2D TTE) and 2D transoesophageal echocardiography (2D TOE). However, these modalities present limitations in detecting vegetations and estimating their dimensions. These disadvantages can be overcome by 3D transoesophageal echocardiography (3D TOE), particularly with the multiplanar reconstruction tool, which allows for the visualization of infinite valve planes, thus optimizing the detection of lesions and precise measurements. Furthermore, the volume rendering provides insight into the anatomical relationships between lesions, which is particularly useful for surgical planning. In this review, we aim to discuss the role of this recent imaging modality in the diagnosis, prognosis, and therapeutic of IE. Finally, we present a collection of images that illustrate the use of 3D TOE tools.

* Corresponding author. E-mail: eliale123@hotmail.com

Graphical Abstract

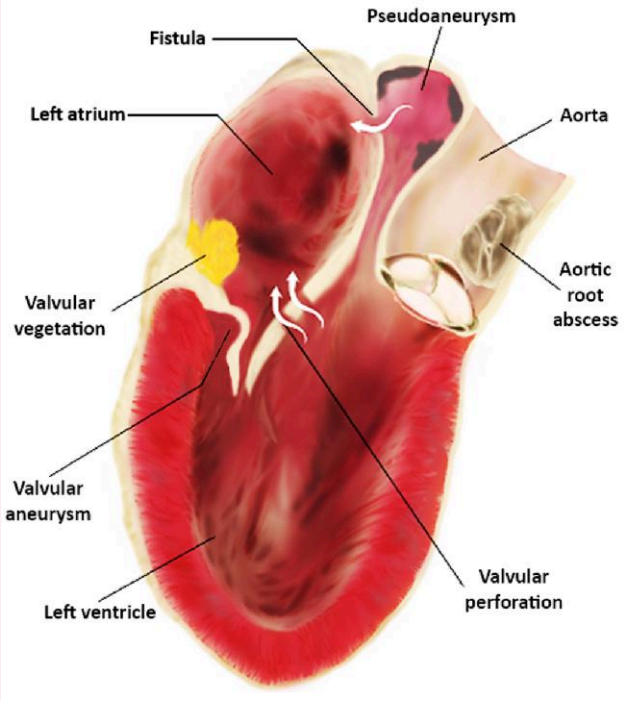

Lesions in IE.

Keywords echocardiography • 3D echocardiography • transoesophageal echocardiography • infective endocarditis

Introduction

Infective endocarditis (IE) is a rare condition classically affecting cardiac valves, currently extending to the infection of intracardiac devices.[1–4] The annual incidence of this condition can reach 10 cases per 100 000 individuals, while in developed countries, the mortality rate is approximately 30% despite advances in its treatment.[5] In the contemporaneous era, we are experiencing an epidemiological transition, which is primarily attributable to more invasive healthcare attention, such as the utilization of cardiac implantable electronic devices and transcatheter interventions. These factors account for 25–30% of cases, as evidenced by recent cohort studies.[3,4,6,7]

From a pathological perspective, microorganisms colonize the valvular endocardial surface, resulting in the formation of vegetations (platelet aggregates, fibrin, inflammatory cells, and microorganisms). Simultaneously, and to varying degrees, a process of tissue destruction occurs leading to perforation, abscess formation, pseudoaneurysm, aneurysm, fistulas, and even suture dehiscence in the case of prostheses (*Graphical Abstract*).[8] These findings are typically detected through 2D transthoracic echocardiography (2D TTE) and/or 2D transoesophageal echocardiography (2D TOE), both of which constitute the cornerstone in the diagnosis of IE.[9,10] However, there are limitations to these techniques that can lead to delays in the detection of lesions, which can be detrimental in a devastating disease such as this one.[9]

In this regard, 3D transoesophageal echocardiography (3D TOE) and especially the multiplanar reconstruction (MPR) tool allow us to improve the identification, morphostructural characterization, and measurement of endocarditis lesions than can be visualized in unlimited planes. On the other hand, volume rendering allows us to obtain highly realistic images of IE lesions, which helps us to typify them and understand their spatial relationship within the heart. Therefore, this complete information is crucial for diagnosis, prognosis, and surgical planning (*Table 1*).[11–15]

The aim of this document is to describe the role of 3D TOE and its tools in different types of endocarditis lesions, for which a systematic literature search using electronic databases was performed. This paper presents the offline processing of a case collection.

2D TTE/2D TOE in IE

2D TTE and 2D TOE are the most commonly used and determinant imaging modalities in the diagnosis of IE. 2D TTE is the first-line modality for detecting IE lesions, assessing valvular structural and functional damage, and determining biventricular size and function.[9,16,17] However, 2D TTE has difficulties in detecting small vegetations, perivalvular complications, and lesions in prosthetic valves or implanted cardiac devices and in providing sufficient morphostructural characterization.[9,11,16,17] For these reasons, 2D TOE should be performed after 2D TTE in all scenarios of suspected or diagnosed IE, except in cases where the clinical suspicion is low.[11]

Several studies have reported the diagnostic superiority of 2D TOE over 2D TTE in the detection of native valve endocarditis (sensitivity, 90–100% vs. 55–90%; specificity, >90% vs. 90%).[5,16–18] These differences are explained by suboptimal acoustic windows in the transthoracic approach (due to obesity, chronic lung pathology, or other thoracic defects), the higher temporal-spatial resolution of 2D TOE [allowing detection of small masses (up to 1 mm) in motion], and the proximity of the oesophageal transducer to the heart.[16,19–21]

Table 1 Ultrasound modalities in IE

	Advantages	Disadvantages	Indications
2D TTE	• Accessible • Non-invasive • Provides functional and haemodynamic data	• Acoustic window • Lower spatial resolution compared with 2D TOE	• First-line test in diagnosis
3D TTE	• Non-invasive • Improved characterization of lesions	• Acoustic window • Lower spatial resolution compared with 3D TOE • Not accessible in all centres • Does not improve detection of endocarditis	• Typification of endocarditis lesions in 2D TOE contraindication
2D TOE	• Better definition of cardiac structures • Higher sensitivity and specificity for small vegetations	• Semi-invasive	• Test that should continue to 2D TTE, except in cases of low clinical suspicion
3D TOE	• Improved detection of vegetations and characterization of lesions • Enhanced precision in measuring maximum vegetation length • Increased detection of perivalvular pathology • Surgery planification	• Not accessible in all centres • Semi-invasive	• Non-conclusive diagnosis with 2D TOE • Determine dimensions accurately • Suspicion of perivalvular lesions or complex pathologies

A similar scenario occurs in prosthetic valve endocarditis, where 2D TTE showed low sensitivity (36–69%), whereas 2D TOE demonstrated sensitivity and specificity > 85%.[19,22]

Despite the high diagnostic performance of 2D TOE in the study of IE, it has certain disadvantages, such as a restricted acquisition to some planes of a volumetric structure, limited data acquisition when procedure speed is required, and usually underestimated vegetation sizes, which in combination could affect lesion detection and embolic risk prediction.[23–25] This performance is even lower when the operator is not an expert echocardiographer, as demonstrated in a recent study that found cardiologists or novices obtained vegetation measurements with greater variance than experienced operators.[26] Additionally, planar images do not facilitate surgical planning as volumetric images do. All these drawbacks are overcome by 3D TOE,[11,12,15,27,28] which becomes a complementary and highly useful test for the diagnosis and surgical planning of IE.

Finally, it is important to mention that 3D transthoracic echocardiography can better characterize endocarditis lesions than 2D transthoracic approach in good acoustic windows. However, it does not increase the detection of this disease in comparison with 2D TTE and has a lower image quality than 2D TOE.[2,14]

Introduction to 3D TOE

3D TOE is a recent modality of transoesophageal ultrasound that involves volumetric acquisition and analysis of a cardiac structure of interest. The entire volume can be acquired in one cardiac cycle or in multiple cycles (multiple sub-volumes that add up to one volume), depending on the desired spatial and/or temporal resolution. The increased ability to discriminate small structures requires the use of a higher number of cycles, which requires a fixed heart rate and controlled breathing.[11,12]

Offline processing or data analysis is as important as data acquisition, and it provides two main final products:

(A) Volume rendering: 3D views with high realism of a structure of interest, providing information about its anatomical relationships. Techniques such as transillumination and transparency enhance the sense of three dimensionality.[11,12]

(B) Unlimited planar images: derived from a MPR of the acquired volume, these are valuable for detecting and characterizing the morphostructural features of specific structures.[11,12,15,23] In addition, tracing the area of the vena contracta helps to assess the severity of valvular regurgitation.[11,12]

An important aspect regarding the matrix array transducer (3D) is its ability to provide two simultaneous planes in real time, which allows the acquisition of unconventional 2D images, shortens the procedure time, and is of paramount importance in structural interventions.[11]

The primary application of 3D TOE in the field of IE results in the following:

- Volumetric images from different perspectives of IE lesions, allowing the typing of the lesions and demonstrating their spatial relationships within the heart[11,17,29,30]
- Unlimited 2D image acquisition, maximizing vegetation detection, length assessment, and precise lesion characterization[16,17,23,24]

Lesions of endocarditis

Vegetations

Vegetations are typical and common lesions of IE, and their dimensions determine the indication for surgery to reduce embolic risk.[9] They consist of heterogeneous echogenic formations with a filiform, sessile, or clustered morphology that are usually attached to the valves and show independent movement.[16,24,31] In the mitral valve, they tend to adhere to the atrial side of the leaflets with movement towards the left atrium during systole, whereas in the aortic valve, they adhere to

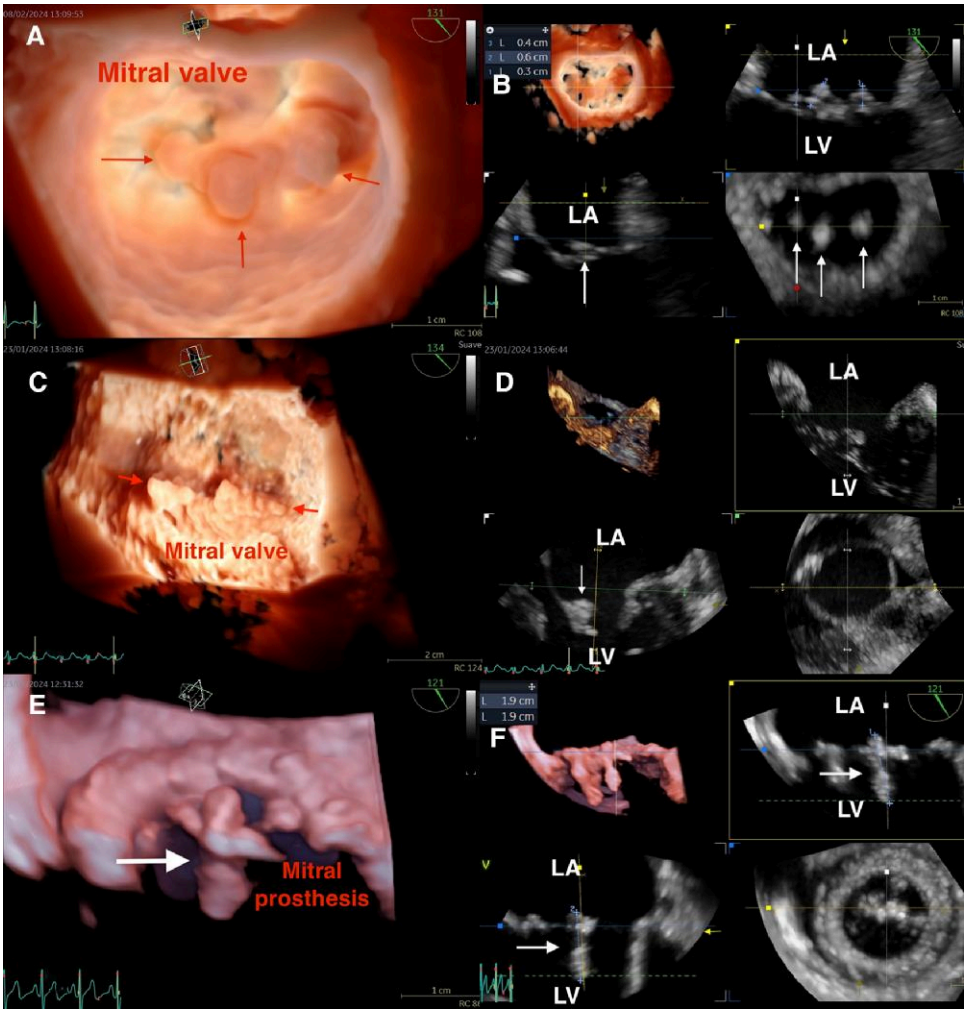

Figure 1 Vegetations. (*A*) TOE at mid-oesophageal level acquired at 131°, volume rendering with transillumination. View in face of the closed mitral valve, showing three ovoid vegetations (red arrows) (*Video 1*). (*B*) MPR of the previous image, locating vegetations in A1, A2, and P3 (white arrows), with the central one being the longest at 6 mm in length. (*C*) TOE at mid-oesophageal level acquired at 134°, volume rendering with transillumination. Surgeon's view of the mitral valve shows sessile vegetations along the intercommissural line (red arrows). (*D*) MPR of the previous case, showing moderate thickening of medial scallops (bottom left quadrant), with the presence of vegetation at the A2 level (white arrow). (*E*) TOE at mid-oesophageal level acquired at 121°, volume rendering of mitral bioprosthetic valve. Medial section of the prosthesis shows filamentous vegetation longitudinally traversing the prosthesis (white arrow). (*F*) MPR of the previous volume, displaying maximum lengths in different views (white arrows). LA, left atrium; LV, left ventricle.

the ventricular side of the leaflets protruding into the outflow tract during diastole.[32]

The technical superiority of 3D TOE over 2D TOE allows for better vegetation detection, accurate morphospatial characterization (number, location, morphology, consistency, mobility, and relationship to the valve structure), and more precise measurement of their maximum lengths. This information is crucial in the diagnostic process, prognostic evaluation, and treatment decision-making.[13,23,24,25,33,34] Similarly, a better ability to detect vegetations in prosthetic valves has been demonstrated with this modality.[13,35–37]

The dimensions of the vegetations have a direct impact on the prediction of embolization, so that patients with vegetations > 10 mm and an embolic event or valve dysfunction should be recommended for urgent surgery.[9,23,25,32,38] It is worth mentioning that patients with vegetations > 30 mm have a high risk of neurological events.[9] When comparing 2D and 3D images, one study identified the best cut-off point at 17 mm for maximum length using 3D TOE and ≥15 mm for 2D TOE, demonstrating better diagnostic accuracy with the former (78% vs. 65%, respectively).[24] Therefore, the application of dimensions derived from 3D images in current management guidelines could lead to surgery in a greater proportion of patients. Regarding tricuspid vegetations, they are better characterized by 3D TOE than by 2D,[39–41] and a maximum length of >16.4 mm strongly predicts septic pulmonary embolism.[42]

It is worth noting that this superior diagnostic performance is achieved using the MPR tool of the 3D software, which analyses planar images. In contrast, the sensitivity of 3D TOE is lower than 2D when using volume rendering images (94% vs. 63%),[17] which is explained by the lower spatial resolution of the 3D image compared with 2D. Therefore, measuring structures in volume rendering images is not recommended (*Figures 1–3*; *Videos 1* and *2*).

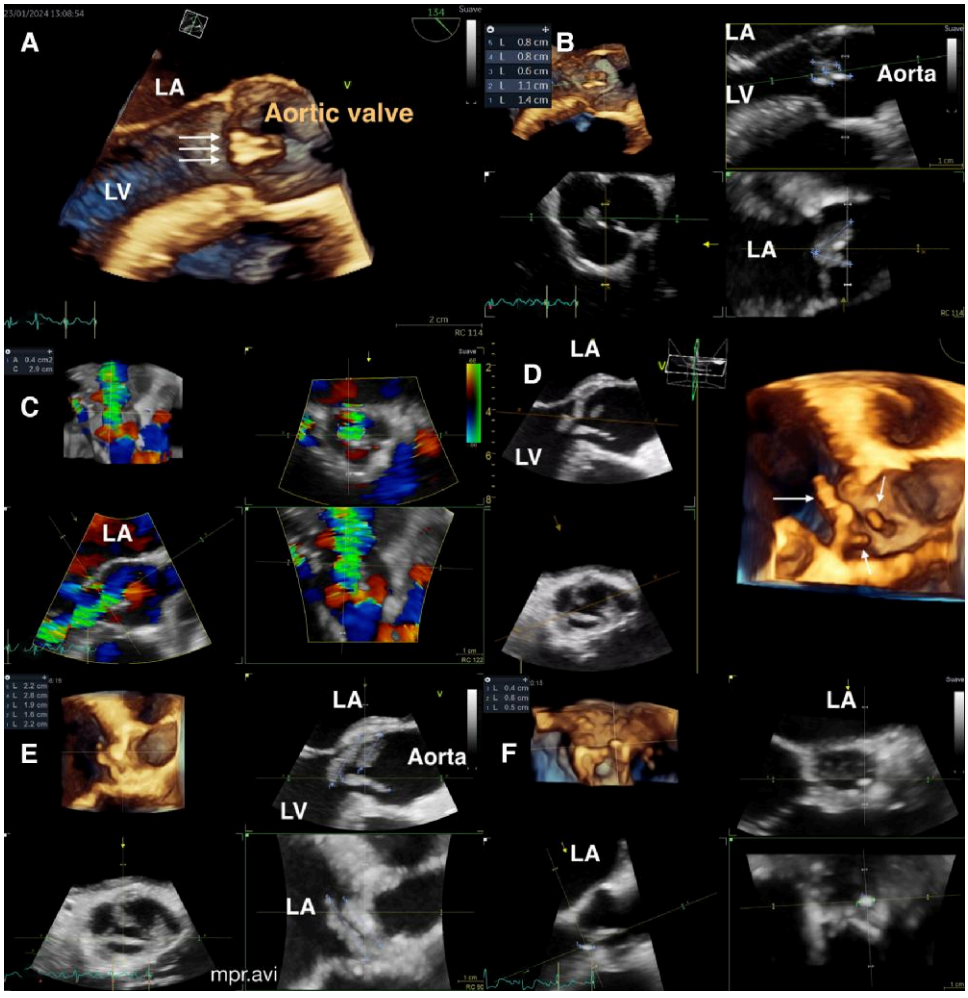

Figure 2 Vegetations. (*A*) TOE at mid-oesophageal level acquired at 134°, volume rendering. Long-axis view of the native aortic valve shows three filamentous vegetations (white arrows). (*B*) MPR of the previous image, locating vegetations on three leaflets, with the non-coronary cusp-dependent one being the largest at 14 mm (bottom right quadrant). (*C*). Colour Doppler MPR of the same case, determining the area of major regurgitation jet at 0.4 cm^2 in the short-axis view (top right quadrant). (*D*) TOE at mid-oesophageal level acquired at 120°, volume rendering. Section and superior view of the native aortic valve shows multiple vegetations (white arrows) distorting the valve. (*E*) MPR of the previous image locates vegetations on all three leaflets and identifies the largest vegetation of 28 mm embedded in the left coronary cusp. (*F*) TOE at mid-oesophageal level acquired at 45°, MPR of the native aortic valve, showing a small ovoid vegetation of 6 mm maximum diameter on the right coronary cusp. LA, left atrium; LV, left ventricle.

Device-related endocarditis

Pacemaker, resynchronization device, or cardioverter-defibrillator leads are associated with IE in less than 1% of cases.[16] 2D TTE has low sensitivity and specificity for the detection of lead vegetations; therefore, transoesophageal approach is recommended, which allows for more detailed characterization of valvular involvement.[43] Benign thrombi on the leads should not be confused with vegetations[44]; we believe that the absence of suggestive images of vegetations and the clinical context are useful to differentiate them. 3D tools such as simultaneous biplanar images allow us to visualize the course of the leads in two planes, including their passage through the tricuspid valve, which in our opinion better detects the presence of vegetations. Finally, large acquired volumes allow panoramic views of longer segments of pacing leads, increasing the probability of visualizing vegetations on the leads.[16]

Perivalvular abscess

Perivalvular abscesses were found at autopsy in 37% of patients with IE and are more common in prosthetic aortic valves with extension to the mitroaortic fibrous tissue.[31,45] In mitral involvement, they are often located in the posterior or lateral aspect of the annulus.[31] This condition leads to complications such as electrical disturbances, fistulization, pericardial disease, and myocardial ischaemia,[46] which significantly worsen the prognosis, especially in the presence of native or prosthetic valve dysfunction.[47]

The sensitivity and specificity for the diagnosis of perivalvular abscess have been estimated at 28 and 98% for 2D TTE and 87 and 95% for 2D TOE, respectively.[45] In a recent study, the MPR tool demonstrated 100% sensitivity in detecting all lesions in 15 perivalvular abscess patients undergoing surgery, while the 2D approach detected only one case, demonstrating better 3D performance.[48] Regarding

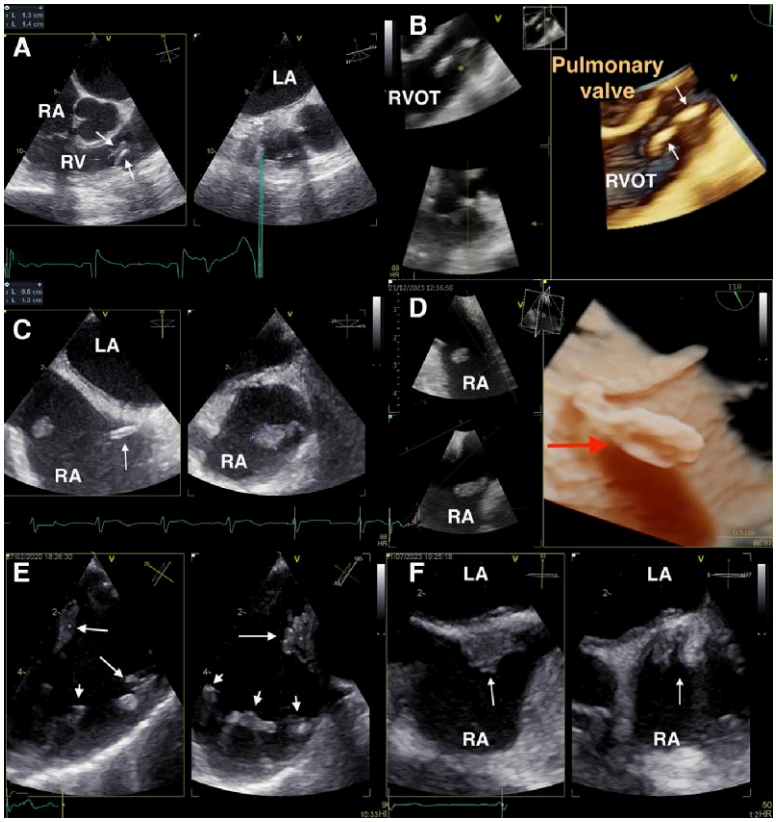

Figure 3 Vegetations. (*A*) TOE at mid-oesophageal level acquired at 74°, simultaneous biplane imaging. Pulmonary valve affected by two filamentous vegetations (white arrows), the largest being 14 mm in length. (*B*) Volume rendering of the pulmonary valve from the previous case, showing filamentous vegetations with enhanced realism. (*C*) TOE at mid-oesophageal level acquired at 88°, simultaneous biplane imaging. Right atrial focus. In the first view, a vegetation is seen near the inferior vena cava ostium and part of the central venous catheter trajectory (white arrow). In the second image, a pedunculated vegetation of 13 mm in diameter is visible (*Video 2*). (*D*) Volume rendering with transillumination of the same patient, showing vegetation with digitiform morphology (red arrow). (*E*) TOE at mid-oesophageal level acquired at 35°, simultaneous biplane imaging. Pulmonary artery trunk focus. Multiple clustered vegetations are shown in the pulmonary artery trunk (long white arrows). Additionally, numerous vegetations are implanted at the level of the pulmonary valve (short white arrows). (*F*) TOE at mid-oesophageal level acquired at 93°, simultaneous biplane imaging. Interatrial septum focus. A vegetation with a broad base, inserted at the fossa ovalis on the right atrial aspect, is evident (white arrows). The central venous catheter was removed in the previous days. LA, left atrium; RA, right atrium; RV, right ventricle; RVOT, right ventricular outflow tract.

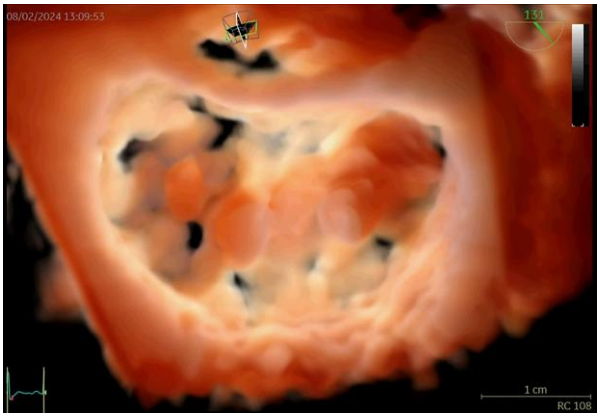

Video 1 TOE 131°, volume rendering with transillumination. View in face of the mitral valve, showing three ovoid vegetations.

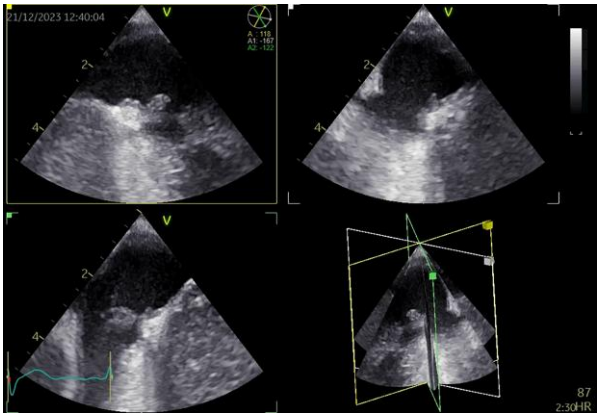

Video 2 TOE 118°, triplanar view. Filiform vegetation inserted near the mouth of the inferior vena cava.

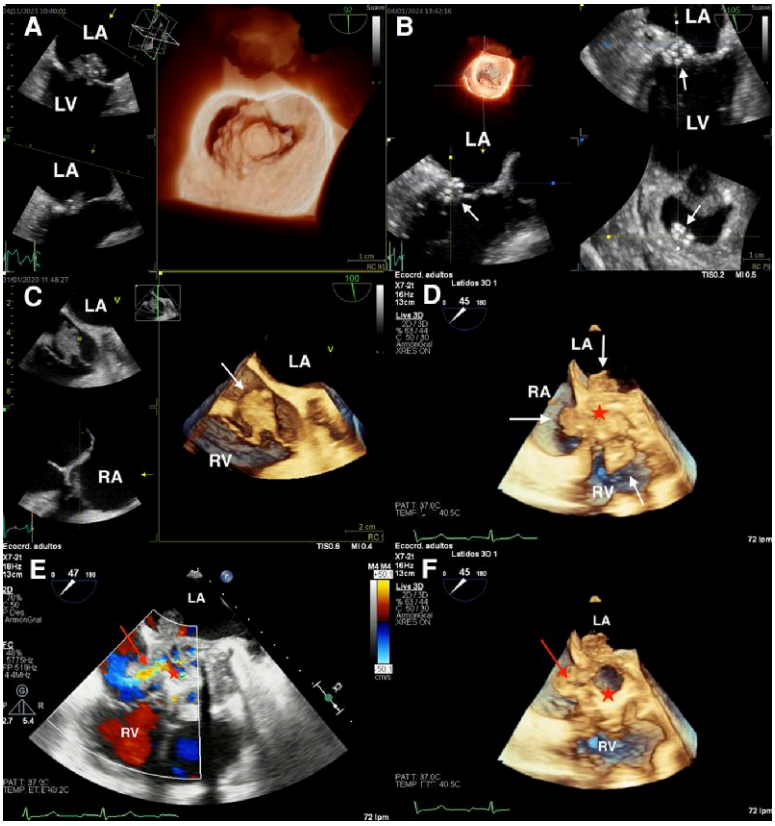

Figure 4 Abscess and fistula. (*A*) TOE at mid-oesophageal level acquired at 92°, volume rendering with transillumination. Mitral valve with a large central image compromising the lateral and medial leaflets, corresponding to a mitral abscess. (*B*) TOE at mid-oesophageal level acquired at 105°, MPR of the mitral valve showing an abscess of the mitral annulus adjacent to P1–P2 (white arrows) (*Video 3*). (*C*) TOE at mid-oesophageal level acquired at 100°, volume rendering. Tricuspid valve focus, showing large abscesses in the septal and anterior leaflets, fused in systole (white arrow). (*D*) TOE at mid-oesophageal level acquired at 45°, volume rendering. Aortic prosthesis focus, revealing a giant abscess arising from the aortic position (red star) and extending with vegetations to the right cavities and left atrium (white arrows). (*E*) TOE at mid-oesophageal level acquired at 47°, 2D with colour Doppler, image from the same study. Biological aortic prosthesis focus, showing a fistulous tract (red arrow) from the aortic pseudoaneurysm abscess (red star) to the right atrium (*Video 4*). (*F*) TOE at mid-oesophageal level acquired at 47°, volume rendering, continuation of the previous image. Aortic pseudoaneurysm abscess (red star) communicating with the right atrium via a fistula (red arrow) (*Video 5*). LA, left atrium; RA, right atrium; LV, left ventricle; RV, right ventricle.

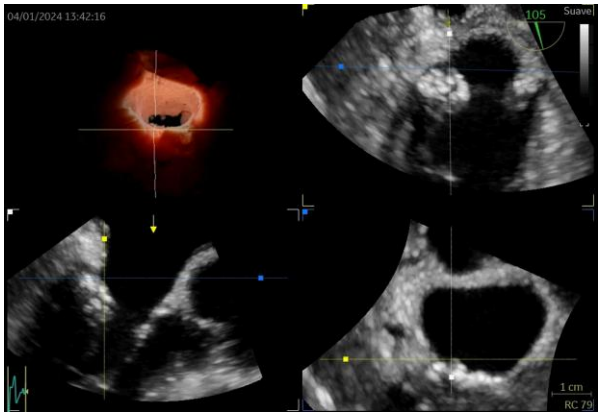

Video 3 TOE 105°, MPR of the mitral valve showing an abscess of the mitral annulus adjacent to P1–P2.

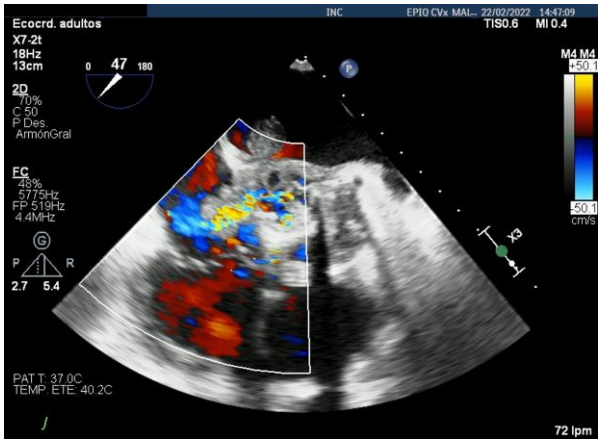

Video 4 TOE 47°, 2D with colour Doppler. Biological aortic prosthesis focus, showing a fistulous tract from the aortic pseudoaneurysm abscess to the right atrium.

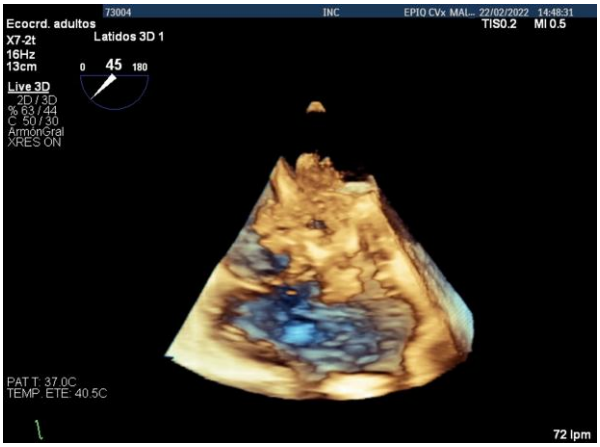

Video 5 TOE 45°, volume rendering. Aortic pseudoaneurysm abscess communicating with the right atrium via a fistula.

cardiac computed tomography (CT), one study found better diagnostic performance than 2D TOE in the detection of perivalvular abscesses, which was attributed to the possibility of complete planar exploration.[20]

3D TOE is useful when conventional tools have equivocal findings because it provides a comprehensive characterization of the abscess (location and size) and details its true extent, which are sometimes missed on routine 2D views.[16,49,50] It is worth noting that this additional information is also valuable for surgical planning[30,51] (*Figure 4*; *Video 3*).

Intracardiac fistulas

Intracardiac fistulas result from perforation of an abscess or pseudoaneurysm associated with native or prosthetic valve endocarditis. The pressure gradient between the communicating chambers produces turbulence on colour Doppler, a useful indirect sign for diagnosis[16] (*Figure 4E*; *Video 4*). The volume rendering of 3D TOE provides realistic images that clarify the complex fistulous tract seen on 2D TOE (*Figure 4F*; *Video 5*). Finally, this information is useful for surgical planning.[52,53]

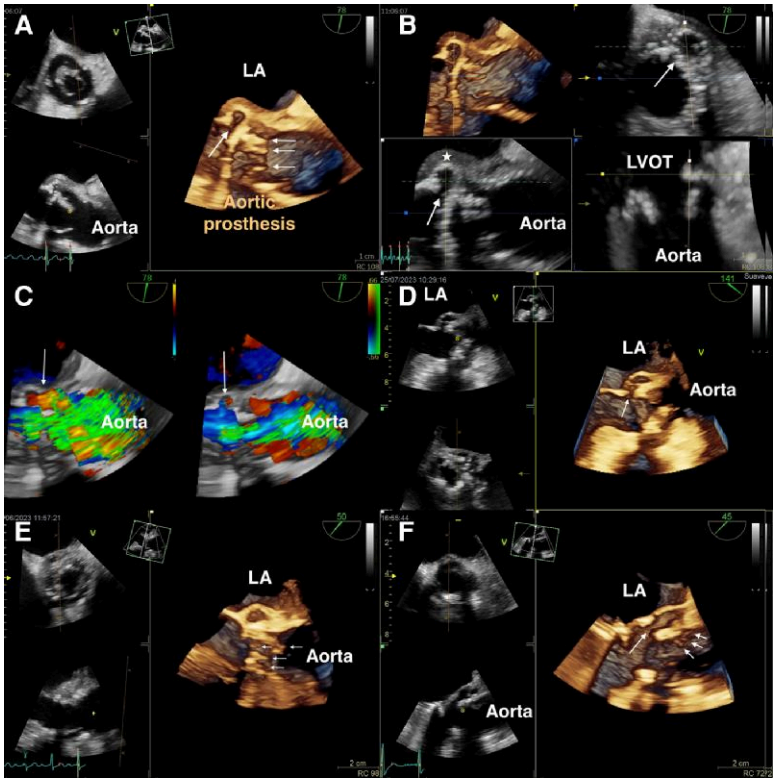

Figure 5 Pseudoaneurysm. (*A*) TOE at mid-oesophageal level acquired at 78°, volume rendering. Biological aortic prosthesis with evidence of pseudoaneurysm of the mitroaortic fibrosa (white arrow) communicating with the left ventricular outflow tract. Additionally, multiple vegetations are visible inside it (thin white arrows). (*B*) MPR of the previous case, showing the pseudoaneurysm in short and long axes, and thickening of the containing wall, corresponding to an abscess (white star). (*C*). Volume rendering with colour Doppler of the same patient. Non-simultaneous biplanar images show flow passage from the aorta to the cavity (white arrow, left image) and from the cavity to the left ventricular outflow tract (white arrow, right image). (*D*) TOE at mid-oesophageal level acquired at 141°, volume rendering. Biological aortic prosthesis focus, showing pseudoaneurysm of the mitroaortic fibrosa (white arrow) connected to the left ventricular outflow tract. It is important to note the thickening of the leaflets. (*E*) TOE at mid-oesophageal level acquired at 50°, volume rendering. Biological aortic prosthesis focus, showing pseudoaneurysm of the mitroaortic fibrosa with thickened lining, and additionally, multiple vegetations are appreciated in the prosthetic arterial aspect. (*F*) TOE at mid-oesophageal level acquired at 45°, volume rendering. Biological aortic prosthesis focus, showing pseudoaneurysm of the mitroaortic fibrosa communicating with the left ventricular outflow tract (long white arrow), and small vegetations are also visible inside it (small white arrows). Note the presence of a mechanical mitral prosthesis. LA, left atrium; LVOT, left ventricular outflow tract.

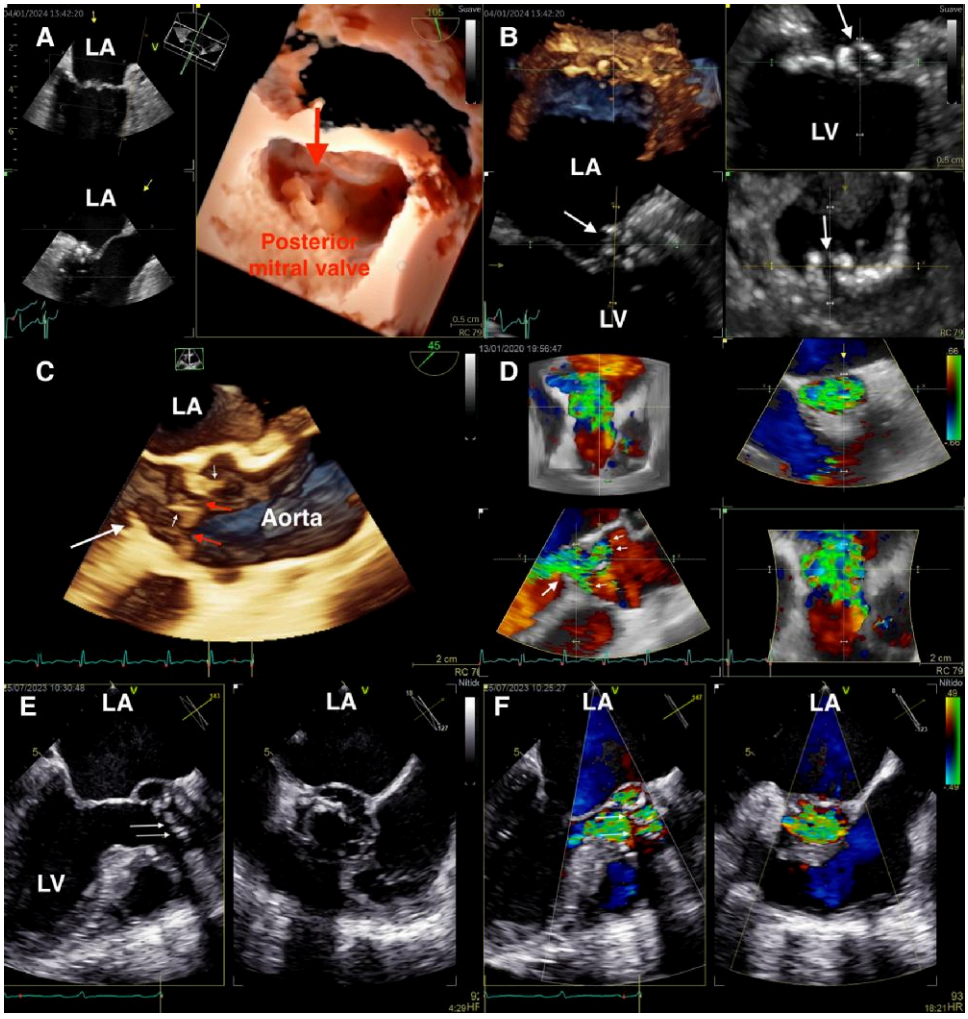

Figure 6 Perforations. (*A*) TOE at mid-oesophageal level acquired at 105°, volume rendering with transillumination. Oblique atrial view of the mitral valve. A perforated aneurysm is observed in the posterior mitral leaflet (*Video 6*). (*B*) MPR of the same case, showing the perforated aneurysm located in P2 in multiple views. (*C*) TOE at mid-oesophageal level acquired at 45°, volume rendering. Native aortic valve with multiple small vegetations (small white arrows) and two perforations in the non-coronary and right leaflets (red arrows). Note the presence of a subaortic membrane (large white arrow). (*D*) MPR with colour Doppler of the previous study, showing multiple perforations (small white arrows) causing severe aortic insufficiency. Regurgitant jet with restricted trajectory due to subaortic membrane (large white arrow). (*E*) TOE at mid-oesophageal level acquired at 143°, simultaneous biplanar image. Biological aortic prosthesis with evidence of multiple fenestrations in its leaflets (white arrows). (*F*) Biplanar image with colour Doppler of the previous image, highlighting multiple non-eccentric regurgitant jets (white arrows) almost completely occupying the left ventricular outflow tract (*Video 7*). LA, left atrium; LV, left ventricle.

Pseudoaneurysm of the mitral-aortic intervalvular fibrosis

A pseudoaneurysm is an anechogenic perivalvular cavity in communication with the bloodstream that expands during systole and collapses during diastole.[54] It is typically the natural progression of an aortic root abscess and can be complicated by rupture into the left atrium, aorta, left ventricle, and pericardial space, which can lead to cardiac tamponade.[16]

As with the other complications mentioned above, TOE is a better tool for evaluating pseudoaneurysms than TTE.[16,55] With regard to 3D TOE, it better detects pseudoaneurysms and accurately describes their relationship to the origin of the proximal coronary arteries.[47,56–60] In addition, this tool accurately localizes the lesion and determines the site of rupture,[11,12,30] making it a very useful technique for surgical planning (*Figure 5*).

Leaflet perforation

This is a destructive lesion of the valve leaflets causing acute regurgitation. This complication is suspected in the presence of an eccentric regurgitant jet away from the coaptation line or in the presence of multiple regurgitant jets without apparent cause.[61] It is more common in the mitral valve than in the aortic valve, and in one-third of cases,

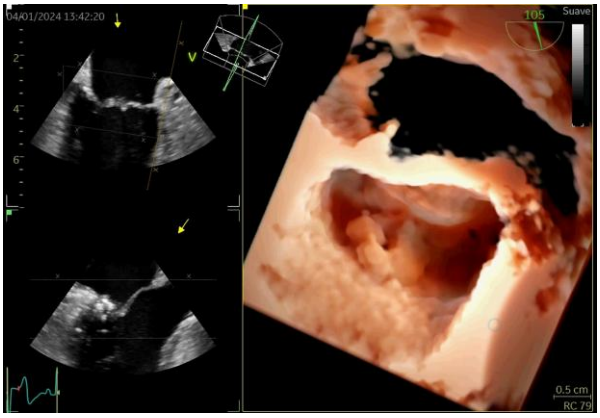

Video 6 TOE 105°, volume rendering with transillumination. Oblique atrial view of the mitral valve. A perforated aneurysm is observed in the posterior mitral leaflet.

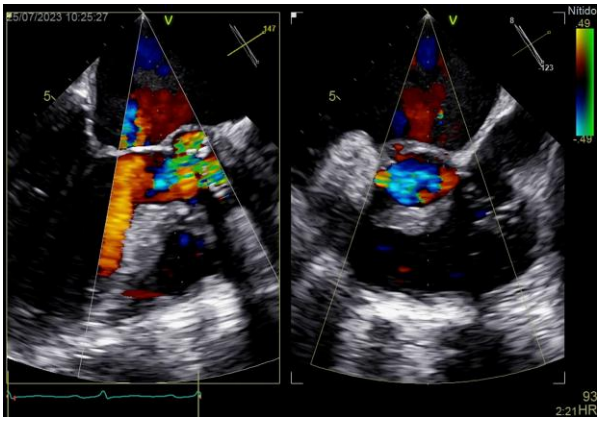

Video 7 TOE at mid-oesophageal level acquired at 147°, simultaneous biplanar image. Biological aortic prosthesis with evidence of multiple fenestrations in its leaflets. Colour Doppler highlighting multiple non-eccentric regurgitant jets almost completely occupying the left ventricular outflow tract.

the perforation is due to a mitral aneurysm.[16,62,63] TOE is the preferred technique over TTE due to its higher sensitivity and specificity (95% vs. 45% and 98% vs. 95%, respectively).[64] However, sometimes the presence of a perforation cannot be detected. In a large retrospective series of cases of valvular perforation, 3D TOE was able to identify four cases of valvular perforation that were not detected by 2D TOE.[65] The superiority of 3D TOE has been attributed to the visualization of anatomical views facing the leaflets, allowing for precise characterization of the shape and location of valvular perforations, which are relevant data for preoperative planning[66,67] (*Figure 6*; *Videos 6 and 7*).

Aneurysms

Valvular aneurysms secondary to IE are a serious and rare complication, mainly affecting the left valves.[16] It is defined as a sac-like bulge in the valvular tissue resulting from weakened valvular tissue due to the inflammatory process. In the case of mitral valve involvement, it is usually associated with aortic insufficiency due to endocarditis.[54,68] They are often complicated by perforations.[30] The first diagnostic tool is TTE, but it has a low sensitivity (42%), so it has to be complemented with TOE. Volume rendering provides maximum image realism and the possibility of better anatomical characterization[69,70] (*Figures 7A–D*; *Video 8*).

Suture dehiscence

Suture dehiscence is characterized by separation of the prosthetic valve from the native annulus due to rupture of the suture. Echocardiographically, it is seen as a space between the native annulus and the suture ring and, in more severe cases, may be seen as a rocking motion.[71]

The aortic valve is more commonly affected due to the presence of less rigid collagenous annular tissue and the absence of a true annulus. Dehiscence most commonly affects the non-coronary sinus.[71] 3D TOE studies localize mitral valve defects more frequently in the posterior and lateral aspects of the mitral annulus. In terms of severity, when the extent of dehiscence exceeds 40% of the prosthetic annulus, prosthesis rocking can cause severe regurgitation and congestive heart failure[49] (*Figure 7E and F*; *Video 9*).

Non-bacterial thrombotic endocarditis (Libman–Sacks)

Non-bacterial thrombotic endocarditis, also known as Libman–Sacks endocarditis, thrombotic or verrucous endocarditis, is a rare form of non-infectious endocarditis that is often unrecognized or misdiagnosed.[72] Typical vegetations may appear as hyperechoic verrucous nodules of reduced size (<1 cm) with broad base, usually on the left valves, preferably the posterior mitral leaflet. Alternatively, they may manifest as diffuse valvular thickening[73,74]; both forms are reversible with immunosuppressive treatment. A recent study comparing 2D TOE and 3D TOE in this scenario showed that the 3D approach detected a higher number of vegetations, provided a better characterization of the vegetations, showed a higher frequency of commissural fusion of affected leaflets or cusps, and, most importantly, detected more vegetations in patients with cerebrovascular disease of cardioembolic origin than 2D TOE.[75] An additional advantage of this test is the ability to better visualize the ventricular aspect of the mitral valve.[76]

Endocarditis associated with congenital heart disease

Endothelial damage due to turbulent flow and the use of intracardiac foreign material in CHD are the main mechanisms leading to IE. In addition, right-sided IE is more common due to greater frictional stress in the right-sided cavities. On the other hand, the presence of complex or multiple defects implies a higher risk of IE than single defects.[3,9] A Japanese cohort of patients with complex congenital heart disease (CHD) who underwent corrective surgery reported low detection of vegetations and abscesses by TTE, suggesting that 2D TOE should be performed in patients with suspected IE associated with CHD.[77] 3D TOE has an undeniable usefulness in the detection of IE associated with CHD in both simple defects and complex anomalies.[78] Obviously, it is of greater relevance in the second scenario, which requires a more detailed evaluation with unlimited planes (MPR) and realistic views from different angles (volume rendering) of the complicated anatomy (*Table 2*).

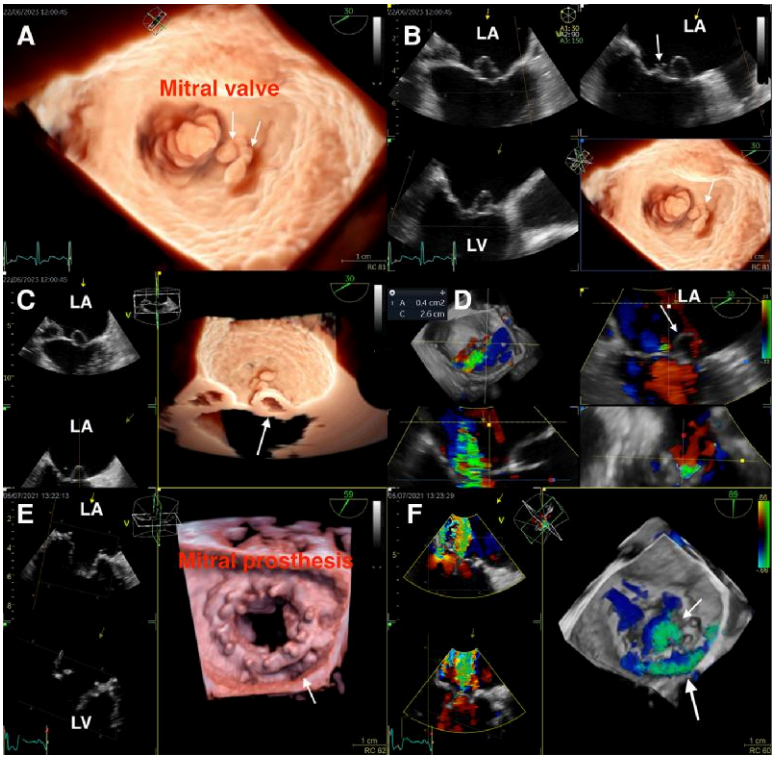

Figure 7 Aneurysm and dehiscence. (*A*) TOE at mid-oesophageal level acquired at 30°, volume rendering with transillumination. Mitral valve in a face view showing an aneurysm involving A1–2, along with two small medial vegetations (white arrows). (*B*) MPR of the previous study showing the profile of the aneurysm in multiple views, as well as its location between the boundary of A1–2. Also, vegetations are localized in A2 (white arrow) (*Video 8*). (*C*) Volume rendering of the same case. Longitudinal section of the mitral aneurysm. (*D*) MPR with colour Doppler of the same patient, displaying the integrity of this cavity in multiple planar views. (*E*) TOE at mid-oesophageal level acquired at 59°, volume rendering. Biological mitral prosthesis in a face view, showing suture dehiscence at the postero-medial level (white arrow) (*Video 9*). (*F*) Volume rendering of the previous case, highlighting a central regurgitant jet (small white arrow) and a larger postero-medial eccentric jet exceeding 25% of the annular circumference (large arrow). LA, left atrium; LV, left ventricle.

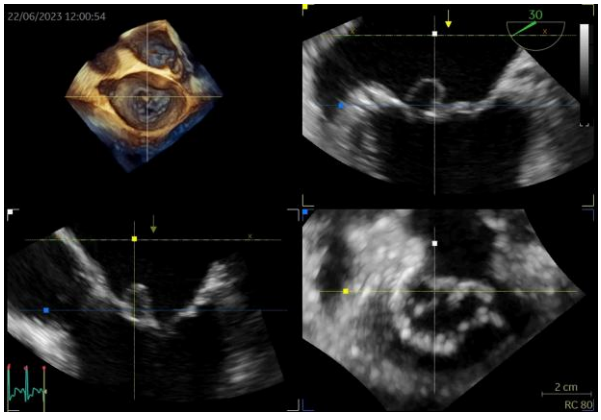

Video 8 TOE 30°. MPR of mitral aneurysm in multiple views, as well as its location between the boundary of A1–2.

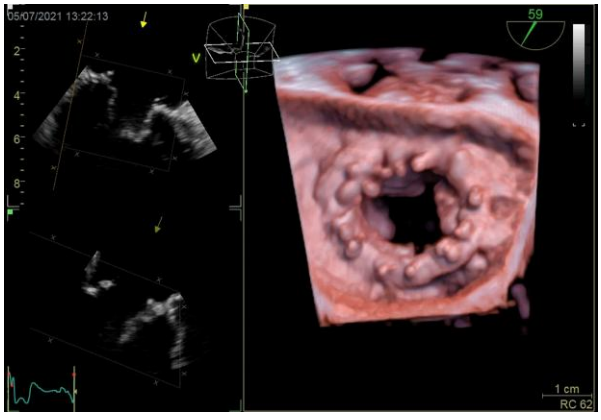

Video 9 TOE 59°, volume rendering. Biological mitral prosthesis in a face view, showing suture dehiscence at the postero-medial level.

Table 2 IE lesions on conventional ultrasound and 3D TOE

	2D echocardiographic characteristics	3D TOE contribution
Vegetations	Filiform, sessile, or grouped intracardiac mass, implanted on a valve or device	MPR improves detection of vegetations, morphospatial characterization, and measurement of their lengths
Device-associated endocarditis	Mobile mass attached to the pacer lead with independent motion	Simultaneous biplane imaging increases vegetation detection
Perivalvular abscess	Thick dense walls, sometimes with echolucent areas which commonly affects the aortic root	MPR increases detection and better defines relationship anatomy for surgical planning
Intracardiac fistulas	Result of ruptured abscess or pseudoaneurysm. Colour Doppler shows continuous flow between two cavities	Volume rendering details fistulous tract useful in surgical planning
Pseudoaneurysm of the mitral-aortic intervalvular fibrosa	Anechogenic perivalvular cavity that communicates with the bloodstream in the fibrous mitro-aorta	MPR better detects this pseudoaneurysm and determines its relationship with the origin of the proximal coronary arteries
Valve leaflet perforation	A small hole in the body of the leaflet, demonstrated with colour Doppler	Detection surpasses 2D, useful in surgical planning
Valve aneurysm	A sac-like lump in the valve tissue that can potentially rupture	Volume rendering provides maximum realism in the images and the possibility of better anatomical characterization
Prosthetic valve dehiscence	Separation of the prosthetic valve from the native annulus due to rupture of the suture line	MPR with colour Doppler precise periprosthetic leak. Volume rendering is useful for surgical planning
Libman–Sacks endocarditis	Small hyperechoic nodules, or diffuse valvular thickening	MPR detects more vegetations
Endocarditis associated with CHD	Vegetations or abscesses in right cavities. Risk of major IE in complex CHD	Volume rendering and MPR more useful in complex or multiple defects

3D TOE limitations

Obtaining images with high spatiotemporal resolution is necessary for better performance of the test; however, this requires technical aspects during the acquisition. Cardiac cycles of equal duration representing sub-volumes and immobilization of the operator–probe–patient unit are necessary for this purpose.[11,12,15]

In addition, artifacts in the 2D image are reflected in the 3D images.[15] Therefore, suboptimally acquired images or those with metal induced artefacts (acoustic shadows and reverberation) may reduce the sensitivity of the test. A multimodal approach is essential in these situations or in the presence of complex pathologies caused by endocarditis. CT is useful in detecting periprosthetic or perivalvular complications, while positron emission tomography (PET/CT) has a high diagnostic yield in detecting prosthetic valve endocarditis.[9]

Finally, the main drawback of this modality is the cost of the equipment, which does not favour the widespread and sustainable development of this useful diagnostic modality.

Conclusions

IE is a devastating heart disease that is increasing in incidence with increasing healthcare interventions. International guidelines recommend imaging studies such as 2D TTE and 2D TOE for the detection of IE lesions. However, technical limitations may delay diagnosis. The 3D TOE emerges as a complementary test with greater accuracy than 2D TOE. It highlights the crucial role of the MPR tool, which maximizes the detection of vegetations and the precision of their dimensions and additionally correctly characterizes endocarditis lesions. Likewise, the volume rendering tool provides realistic images useful for morphospatial characterization, which is essential in complex lesions such as periannular complications in patients with prosthetic valves. In conclusion, 3D TOE in IE is the ultrasound test with the best diagnostic performance, has a greater impact on prognosis, and ultimately facilitates surgical planning.

Conflict of interest: None declared.

Funding

None declared.

Data availability

The data underlying this article are available in the article and in its online supplementary material.

Lead author biography

Roberto Baltodano is a cardiologist at the Guillermo Almenara Hospital and a professor at the San Marcos University in Lima, Peru. He is a past fellow of echocardiography at the Vall de Hebron Hospital in Barcelona and a certified echocardiographer of the ESC; his research interest is advanced echocardiography.

References

1. Miao H, Zhang Y, Zhang Y, Zhang J. Update on the epidemiology, diagnosis, and management of infective endocarditis: a review. *Trends Cardiovasc Med* 2024:S1050-1738(24)00001-X.
2. Hubers SA, DeSimone DC, Gersh BJ, Anavekar NS. Infective endocarditis: a contemporary review. *Mayo Clin Proc* 2020;**95**:982–97.
3. Baddour LM, Wilson WR, Bayer AS, Fowler VGJr, Tleyjeh IM, Rybak MJ *et al.* Infective endocarditis in adults: diagnosis, antimicrobial therapy, and management of

complications: a scientific statement for healthcare professionals from the American Heart Association. *Circulation* 2015;**132**:1435–86.
4. Yew HS, Murdoch DR. Global trends in infective endocarditis epidemiology. *Curr Infect Dis Rep* 2012;**14**:367–72.
5. Cahill TJ, Baddour LM, Habib G, Hoen B, Salaun E, Pettersson GB *et al.* Challenges in infective endocarditis. *J Am Coll Cardiol* 2017;**69**:325–44.
6. Rajani R, Klein JL. Infective endocarditis: a contemporary update. *Clin Med (Lond)* 2020; **20**:31–5.
7. Tornos P, Gonzalez-Alujas T, Thuny F, Habib G. Infective endocarditis: the European viewpoint. *Curr Probl Cardiol* 2011;**36**:175–222.
8. Lung B. Endocardite infectieuse. Épidémiologie, physiopathologie et anatomopathologie [infective endocarditis. Epidemiology, pathophysiology and histopathology]. *Presse Med* 2019;**48**:513–21.
9. Delgado V, Ajmone Marsan N, de Waha S, Bonaros N, Brida M, Burri H *et al.* 2023 ESC guidelines for the management of endocarditis. *Eur Heart J* 2023;**44**:ehad193.
10. Rezar R, Lichtenauer M, Haar M, Hödl G, Kern JM, Zhou Z *et al.* Infective endocarditis—a review of current therapy and future challenges. *Hellenic J Cardiol* 2021;**62**:190–200.
11. Faletra FF, Agricola E, Flachskampf FA, Hahn R, Pepi M, Ajmone Marsan N *et al.* Three-dimensional transoesophageal echocardiography: how to use and when to use-a clinical consensus statement from the European Association of Cardiovascular Imaging of the European Society of Cardiology. *Eur Heart J Cardiovasc Imaging* 2023;**24**:e119–97.
12. Lang RM, Badano LP, Tsang W, Adams DH, Agricola E, Buck T *et al.* EAE/ASE recommendations for image acquisition and display using three-dimensional echocardiography. *Eur Heart J Cardiovasc Imaging* 2012;**13**:1–46.
13. Tomoaia R, Beyer RȘ, Dădârlat-Pop A, Șerban AM, Pop D, Zdrenghea D *et al.* Novel 3D versus traditional transesophageal echocardiography techniques: defining differences in the diagnosis of infective endocarditis. *Eur J Clin Invest* 2024;**54**:e14103.
14. Liu Y-W, Tsai W-C, Lin C-C, Hsu C-H, Li W-T, Lin L *et al.* Usefulness of real-time three-dimensional echocardiography for diagnosis of infective endocarditis. *Scand Cardiovasc J* 2009;**43**:318–23.
15. Poon J, Leung JT, Leung DY. 3D echo in routine clinical practice—state of the art in 2019. *Heart Lung Circ* 2019;**28**:1400–10.
16. Afonso L, Kottam A, Reddy V, Penumetcha A. Echocardiography in infective endocarditis: state of the art. *Curr Cardiol Rep* 2017;**19**:127.
17. Pfister R, Betton Y, Freyhaus HT, Jung N, Baldus S, Michels G. Three-dimensional compared to two-dimensional transesophageal echocardiography for diagnosis of infective endocarditis. *Infection* 2016;**44**:725–31.
18. Bai AD, Steinberg M, Showler A, Burry L, Bhatia RS, Tomlinson GA *et al.* Diagnostic accuracy of transthoracic echocardiography for infective endocarditis findings using transesophageal echocardiography as the reference standard: a meta-analysis. *J Am Soc Echocardiogr* 2017;**30**:639–646.e8.
19. Montané B, Chahine J, Fiore A, Alzubi J, Alnajjar H, Mutti J *et al.* Diagnostic performance of contemporary transesophageal echocardiography with modern imaging for infective endocarditis. *Cardiovasc Diagn Ther* 2023;**13**:25–37.
20. Kim IC, Chang S, Hong GR, Lee SH, Lee S, Ha JW *et al.* Comparison of cardiac computed tomography with transesophageal echocardiography for identifying vegetation and intracardiac complications in patients with infective endocarditis in the era of 3-dimensional images. *Circ Cardiovasc Imaging* 2018;**11**:e006986.
21. Yuan XC, Liu M, Hu J, Zeng X, Zhou AY, Chen L. Diagnosis of infective endocarditis using echocardiography. *Medicine (Baltimore)* 2019;**98**:e17141.
22. Evangelista A, Gonzalez-Alujas MT. Echocardiography in infective endocarditis. *Heart (British Cardiac Society)* 2004;**90**:614–7.
23. Berdejo J, Shibayama K, Harada K, Tanaka J, Mihara H, Gurudevan SV *et al.* Evaluation of vegetation size and its relationship with embolism in infective endocarditis: a real-time 3-dimensional transesophageal echocardiography study. *Circ Cardiovasc Imaging* 2014;**7**: 149–54.
24. Pérez-García CN, Olmos C, Islas F, Marcos-Alberca P, Pozo E, Ferrera C *et al.* Morphological characterization of vegetation by real-time three-dimensional transesophageal echocardiography in infective endocarditis: prognostic impact. *Echocardiography* 2019;**36**:742–51.
25. Sordelli C, Fele N, Mocerino R, Weisz SH, Ascione L, Caso P *et al.* Infective endocarditis: echocardiographic imaging and new imaging modalities. *J Cardiovasc Echogr* 2019;**29**: 149–55.
26. Schmidt L, Østergaard L, Grund FF, Schmidt L, Linde JJ, Køber L *et al.* Importance of experience in transoesophageal echocardiographic evaluation of vegetation size in patients with infective endocarditis: a reliability study. *Eur Heart J Imaging Methods Pract* 2024;**2**:qyae024.
27. Bhattacharyya S, Bahrami T, Rahman-Haley S. Comprehensive assessment of complications of infective endocarditis by 3D transesophageal echocardiography. *Int J Cardiol* 2014;**174**:e87–9.
28. Ahluwalia V, Osman F, Parmar J, Khan JN. 3D echocardiography allows rapid and accurate surgical planning in complex aortic root abscess cases. *Echo Res Pract* 2019;**6**: K23–30.
29. Sedgwick JF, Burstow DJ. Update on echocardiography in the management of infective endocarditis. *Curr Infect Dis Rep* 2012;**14**:373–80.
30. Khan M, De Sousa R, Rai K, Khan JN. Unique characterization of complex endocarditic vegetations using 3D TOE. *Echo Res Pract* 2020;**7**:I5–7.
31. Galzerano D, Kinsara AJ, Di Michele S, Vriz O, Fadel BM, Musci RL *et al.* Three dimensional transesophageal echocardiography: a missing link in infective endocarditis imaging? *Int J Cardiovasc Imaging* 2020;**36**:403–13.
32. Salaun E, Habib G. Beyond standard echocardiography in infective endocarditis: computed tomography, 3-dimensional imaging, and multi-imaging. *Circ Cardiovasc Imaging* 2018;**11**:e007626.
33. Becic T, Perkovic-Avelini R, Fabijanic D. Native mitral valve infective endocarditis: a significant contribution of 3d-transthoracic echocardiography. *Med Ultrason* 2023;**25**: 359–60.
34. Muayed M E, Burjonroppa SC, Croitoru M. Added accuracy with 3D echocardiographic imaging of valvular vegetations. *Echocardiography* 2005;**22**:361–2.
35. González YO, Ung R, Blackshear JL, Laman SM. Three-dimensional echocardiography for diagnosis of transcatheter prosthetic aortic valve endocarditis. *CASE (Phila* 2017;**1**: 155–8.
36. Pasha AK, Snyder BA, Zangeneh TT, Thompson JL, Sobonya RE, Abidov A. A distinctly rare case of candida endocarditis involving the bioprosthetic pulmonary and the Eustachian valve diagnosed on 3D transesophageal echocardiography. *Echocardiography* 2015;**32**:607–9.
37. Sarı C, Durmaz T, Karaduman BD, Keleş T, Bayram H, Baştuğ S *et al.* Prosthetic valve endocarditis 7 months after transcatheter aortic valve implantation diagnosed with 3D TEE. *Hellenic J Cardiol* 2016;**57**:119–23.
38. Asch FM, Bieganski SP, Panza JA, Weissman NJ. Real-time 3-dimensional echocardiography evaluation of intracardiac masses. *Echocardiography* 2006;**23**:218–24.
39. Bandyopadhyay S, Mandana K. Tricuspid valve endocarditis: 3D TEE en face view helps better identification of location and extent of involvement. *Ann Card Anaesth* 2023;**26**: 206–8.
40. Brunetti ND, De Gennaro L, Basile DP, De Cillis E, Acquaviva T, Boscia F *et al.* A "strange cough": 3D-echocardiography for diagnosis of late tricuspid valve endocarditis in a former drug addict with septic pulmonary emboli. *Int J Cardiol* 2011;**153**:e15–8.
41. Naqvi TZ, Rafie R, Ghalichi M. Real-time 3D TEE for the diagnosis of right-sided endocarditis in patients with prosthetic devices. *JACC Cardiovasc Imaging* 2010;**3**:325–7.
42. Utsunomiya H, Berdejo J, Kobayashi S, Mihara H, Itabashi Y, Shiota T. Evaluation of vegetation size and its relationship with septic pulmonary embolism in tricuspid valve infective endocarditis: a real time 3DTEE study. *Echocardiography* 2017;**34**:549–56.
43. Cacoub P, Leprince P, Nataf P, Hausfater P, Dorent R, Wechsler B *et al.* Gandjbakhch I. Pacemaker infective endocarditis. *Am J Cardiol* 1998;**82**:480–4.
44. Korkeila PJ, Saraste MK, Nyman KM, Koistinen J, Lund J, Juhani Airaksinen KE. Transesophageal echocardiography in the diagnosis of thrombosis associated with permanent transvenous pacemaker electrodes. *Pacing Clin Electrophysiol* 2006;**29**:1245–50.
45. Daniel WG, Mügge A, Martin RP, Lindert O, Hausmann D, Nonnast-Daniel B *et al.* Improvement in the diagnosis of abscesses associated with endocarditis by transesophageal echocardiography. *N Engl J Med* 1991;**324**:795–800.
46. Thomas D, Desruennes M, Jault F, Isnard R, Gandjbakhch I. Les abcès cardiaques et extracardiaques dans l'endocardite infectieuse [cardiac and extracardiac abscesses in bacterial endocarditis]. *Arch Mal Coeur Vaiss* 1993;**86**(12 Suppl):1825–35. French.
47. Cosmi JE, Tunick PA, Kronzon I. Mortality in patients with paravalvular abscess diagnosed by transesophageal echocardiography. *J Am Soc Echocardiogr* 2004;**17**:766–8.
48. Tanis W, Teske AJ, van Herwerden LA, Chamuleau S, Meijboom F, Budde RP *et al.* The additional value of three-dimensional transesophageal echocardiography in complex aortic prosthetic heart valve endocarditis. *Echocardiography* 2015;**32**:114–25.
49. Carević V, Mladenović Z, Perković-Avelini R, Bečić T, Radić M, Fabijanić D. Three-dimensional transesophageal echocardiography in the diagnosis and treatment of mitral prosthetic valve endocarditis—a narrative review. *Medicina (Kaunas, Lithuania)* 2021;**58**:23.
50. Iida R, Becher H. Aortic root abscess configuration identified by 3-dimensional echocardiography. *Arch Cardiovasc Dis* 2014;**107**:574–5.
51. Yong MS, Saxena P, Killu AM, Coffey S, Burkhart HM, Wan SH *et al.* The preoperative evaluation of infective endocarditis via 3-dimensional transesophageal echocardiography. *Tex Heart Inst J* 2015;**42**:372–6.
52. Taskesen T, Goldberg SL, Gill EA. Role of three-dimensional echocardiography in management of acquired intracardiac shunts. *Echocardiography* 2014;**31**:E250-3.
53. Gürsoy MO, Özkan M, Aykan AÇ, Yıldız M, Kahveci G. Multimodality imaging of the mitral paravalvular abscess cavity with left ventriculo-atrial fistula. *Heart Lung Circ* 2012;**21**: 284–6.
54. Xie M, Li Y, Cheng TO, Wang X, Lu Q, He L *et al.* Pseudoaneurysm of the mitral-aortic intervalvular fibrosa. *Int J Cardiol* 2013;**166**:2–7.
55. Minamimura H, Ishikawa T, Murakami T, Kotani S. Aortic valve aneurysm associated with infective endocarditis: case report and review of literature. *Gen Thorac Cardiovasc Surg* 2017;**65**:408–14.
56. Kumar P, Kenchappa K, Jena S, Manik G. Ruptured pseudo-aneurysm of the mitral-aortic intervalvular fibrosa—a 3D transesophageal echocardiographic depiction. *J Cardiol Cases* 2017;**15**:161–2.

57. Han J, He Y, Gu X, Sun L, Zhao Y, Liu W *et al.* Echocardiographic diagnosis and outcome of pseudoaneurysm of the mitral-aortic intervalvular fibrosa: results of a single-center experience in Beijing. *Medicine (Baltimore)* 2016;**95**:e3116.
58. Moreno N, Sánchez-Enrique C, Marcos-Alberca P, de Agustín JA, Luengo P, Maroto L *et al.* Large pseudoaneurysm of the mitral annulus as an infective endocarditis complication: a 3D echocardiography role in diagnosis and surgical procedure. *Echocardiography* 2014;**31**: E261–3.
59. Güngör B, Altay S, Dayı SÜ, Bolca O. 3D echocardiographic evaluation of ruptured pseudoaneurysm of the mitral-aortic intervalvular fibrosa. *Anadolu Kardiyol Derg* 2012; **12**:E42–3.
60. Caselli S, Mazzesi G, Tritapepe L, Barretta A, Pandian NG, Agati L *et al.* 3D echocardiographic delineation of mitral-aortic intervalular fibrosa pseudoaneurysm caused by bicuspid aortic valve endocarditis. *Echocardiography* 2011;**28**:E1–4.
61. Wierzbowska-Drabik K, Damian Kasprzak J. Flail, aneurysm, perforation: enhanced visualisation of complex mitral valve damage in enterococcal endocarditis using 3D-echocardiography. *Acta Cardiol* 2018;**73**:101–2.
62. Boumaaz M, Lahjouji MR, Faraj R, Mouine N, Asfalou I, Benyass A. Rare complications of infective endocarditis in marfan-like morphotype: diagnosis of multiple mitral valve aneurysms and aortic root abscess using three-dimensional transesophageal echocardiography. *BMC Cardiovasc Disord* 2024;**24**:51.
63. Lavanco V, Curzi M, Giustiniano E, Raspante D, Di Lisi D, Bragato RM. Perforated giant mycotic aneurysm of mitral valve in a drug-addicted young man: rare complication of infective endocarditis. *Echocardiography* 2018;**35**:129–31.
64. De Castro S, Cartoni D, D'amati G, Beni S, Yao J, Fiorell M *et al.* Diagnostic accuracy of transthoracic and multiplane transesophageal echocardiography for valvular perforation in acute infective endocarditis: correlation with anatomic findings. *Clin Infect Dis* 2000; **30**:825–6.
65. Thompson KA, Shiota T, Tolstrup K, Gurudevan SV, Siegel RJ. Utility of three-dimensional transesophageal echocardiography in the diagnosis of valvular perforations. *Am J Cardiol* 2011;**107**:100–2.
66. Vrettou AR, Zacharoulis A, Lerakis S, Kremastinos DT. Revealing infective endocarditis complications by echocardiography: the value of real-time 3D transesophageal echocardiography. *Hellenic J Cardiol* 2013;**54**:147–9.
67. Cagli K, Gursoy HT, Basyigit F, Koprucu E, Golbasi Z. 3-dimensional images of mitral annulus perforation: an alien's mouth. *JACC Case Rep* 2022;**4**:101681.
68. Janardhanan R, Kamal MU, Riaz IB, Smith MC. Anterior mitral valve aneurysm: a rare sequelae of aortic valve endocarditis. *Echo Res Pract* 2016;**3**:K7–K13.
69. An Y, Chen K, Nie F. Echocardiography diagnosis of mitral valve aneurysm complicated with infective endocarditis. *Int Heart J* 2023;**64**:959–62.
70. Luo Y, Tan H, Wang J, Ye C, Qin. Accurate and rapid diagnosis of complex mitral valve aneurysm with neoplasm via real-time 3D transesophageal echocardiography. *Heart Surg Forum* 2022;**25**:E403–6.
71. Rajiah P, Moore A, Saboo S, Goerne H, Ranganath P, MacNamara J *et al.* Multimodality imaging of complications of cardiac valve surgeries. *Radiographics* 2019;**39**:932–56.
72. Zmaili M, Alzubi J, Lo Presti Vega S, Ababneh E, Xu B. Non-bacterial thrombotic endocarditis: a state-of-the-art contemporary review. *Prog Cardiovasc Dis* 2022;**74**:99–110.
73. Tonutti A, Scarfò I, La Canna G, Selmi C, De Santis M. Diagnostic work-up in patients with nonbacterial thrombotic endocarditis. *J Clin Med* 2023;**12**:5819.
74. Adil A, Kazmi FN, Malik IA, Ammar KA. Severe aortic regurgitation from aortic valve perforation in Libman-Sacks endocarditis: ncremental value of 3D TEE. *Echocardiography* 2022;**39**:1641–2.
75. Roldan CA, Tolstrup K, Macias L, Qualls CR, Maynard D, Charlton G *et al.* Libman-Sacks endocarditis: detection, characterization, and clinical correlates by three-dimensional transesophageal echocardiography. *J Am Soc Echocardiogr* 2015;**28**:770–9.
76. Flint N, Siegel RJ. Libman-Sacks vegetations detected by 3D echocardiography. *Eur Heart J Cardiovasc Imaging* 2018;**19**:292.
77. Niwa K, Nakazawa M, Tateno S, Yoshinaga M, Terai M. Infective endocarditis in congenital heart disease: Japanese national collaboration study. *Heart* 2005;**91**:795–800.
78. Moscatelli S, Leo I, Bianco F, Surkova E, Pezel T, Donald NA *et al.* The role of multimodality imaging in patients with congenital heart disease and infective endocarditis. *Diagnostics (Basel)* 2023;**13**:3638.